

## Supporting Information

### Isomers of terephthalate derivatives as anodes for sodium-ion batteries

Mei Tang ‡, <sup>a,b</sup> Kangkang Jia ‡\*, <sup>a,b</sup> Guandie Ma, <sup>a,b</sup> Fei Wu, <sup>a,b</sup> Yunjie Xiang, <sup>a,b</sup> Qiulin Li, <sup>a,b</sup>  
Qianwei Chen, <sup>a,b</sup> Yuansheng Luo, <sup>a,b</sup> Maowen Xu, <sup>a,b</sup> Shu-Juan Bao\* <sup>a,b</sup>

<sup>a</sup> *School of Materials & Energy, Southwest University, Chongqing 400715, P.R. China.*

<sup>b</sup> *Chongqing Key Laboratory of Battery Materials and Technologies, Chongqing 400715, P.R. China.*

‡ *These authors contributed equally to this work.*

\**Corresponding authors. E-mail addresses: baoshj@swu.edu.cn, kkjia826@163.com;*

## Contents

1. General Methods
2. Experimental Section
3. Spectra and Figures

Fig. S1.  $^1\text{H}$  NMR spectrum of S1 in  $\text{CDCl}_3$ .

Fig. S2.  $^{13}\text{C}$  NMR spectrum of S1 in  $\text{CDCl}_3$ .

Fig. S3.  $^1\text{H}$  NMR spectrum of P- $\text{H}_4\text{TT}$  in DMSO.

Fig. S4.  $^{13}\text{C}$  NMR spectrum of P- $\text{H}_4\text{TT}$  in DMSO.

Fig. S5.  $^1\text{H}$  NMR spectrum of P-TT in  $\text{D}_2\text{O}$ .

Fig. S6.  $^{13}\text{C}$  NMR spectrum of P-TT in  $\text{D}_2\text{O}$ .

Fig. S7.  $^1\text{H}$  NMR spectrum of S2 in  $\text{CDCl}_3$ .

Fig. S8.  $^{13}\text{C}$  NMR spectrum of S2 in  $\text{CDCl}_3$ .

Fig. S9.  $^1\text{H}$  NMR spectrum of M- $\text{H}_4\text{TT}$  in DMSO.

Fig. S10.  $^{13}\text{C}$  NMR spectrum of M- $\text{H}_4\text{TT}$  in DMSO.

Fig. S11. ESI-MS of P- $\text{H}_4\text{TT}$ .

Fig. S12. ESI-MS of M- $\text{H}_4\text{TT}$ .

Fig. S13.  $^1\text{H}$  NMR spectrum of M-TT in  $\text{D}_2\text{O}$ .

Fig. S14.  $^{13}\text{C}$  NMR spectrum of M-TT in  $\text{D}_2\text{O}$ .

Fig. S15. The UV-vis absorption spectra of M-TT and P-TT (solvent, TETRAGLYME=100 Vol%, 25 °C); insets: photographs of M-TT and P-TT electrode-immersed solvents of TETRAGLYME on different days.

Fig. S16. CV curve of a) P-TT and b) M-TT with the pseudocapacitive contribution shown by the shaded regions at a scan rate of  $0.5 \text{ mV s}^{-1}$ .

Fig. S17. The P-TT pellet was obtained by the classic powder's pressing method (18 MPa).

Fig. S18. The M-TT pellet was obtained by the classic powder's pressing method (18 MPa).

Table S1. Electric conductivity results of M-TT and P-TT.

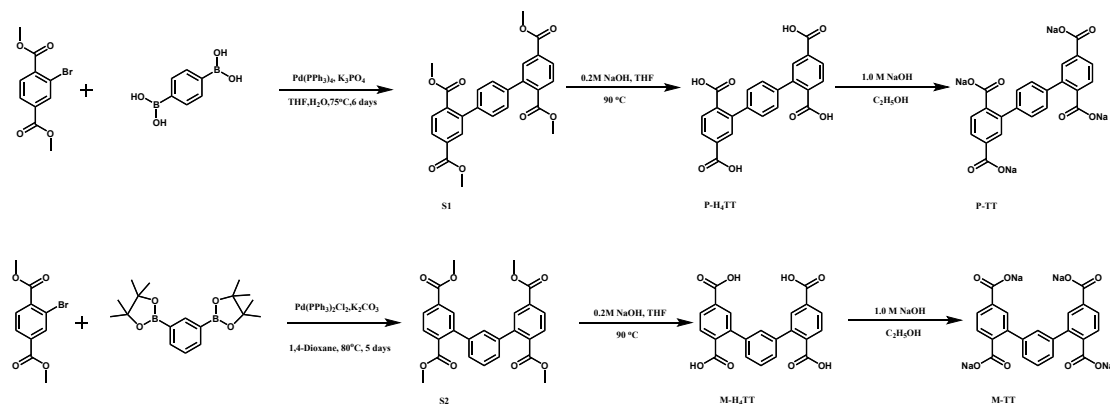
Fig. S19 The electric conductivity of the composite was measured by the four-probe method (Suzhou Jingge Electronics ST2643).

## 1. General Methods

Unless otherwise stated, all starting materials were purchased from commercial suppliers (Sigma Aldrich, Adamas, Acros, and the Energy Chemical) and used without further purification. Dimethyl 2-bromoterephthalate (98%+, Adamas), 1,3-Phenylenediboronic Acid Pinacol Ester (98%+, Adamas), 1,4-Phenylenediboronic acid (98%+, Adamas), Diethyl Carbonate (99%, Acros), N-Methyl-2-pyrrolidinone (99.9%+, Energy Chemical),  $K_3PO_4$  (99%, Adamas),  $Pd(PPh_3)_4$  (99%, Sigma Aldrich), Tetrahydrofuran (THF, 99%, Adamas), NaOH (AR, Greagent), HCl (AR, Chuandong Chemical), Ethanol (AR, Greagent), and anhydrous 1,4-dioxane (99.8%, Sigma-Aldrich) were purchased and used without further purification.

## 2. Experimental Section

### 2.1 Materials Synthetic:



Scheme S1 the synthetic route of compounds *P-TT* and *M-TT*.

#### **Synthesis of tetramethyl [1,1':4',1''-terphenyl]-2,2'',5,5''-tetracarboxylate (S1):**

Dimethyl 2-bromoterephthalate (1000.0 mg, 3.7 mmol), 1,4-Phenylenediboronic acid (275.9 mg, 1.7 mmol), and  $\text{K}_3\text{PO}_4$  (1225.8 mg, 5.8 mmol) were mixed in a 100 mL Schlenk flask. After added  $\text{Pd}(\text{PPh}_3)_4$  (95.3 mg, 0.1 mmol) in the glove box, then add anhydrous THF-water (15.0 mL, 7.0 mL). The mixture was heated to reflux or a week under an Ar atmosphere. Stop the reaction after a solid precipitate, wash with water and petroleum ether, and filter. Recrystallization from methanol offered the pure tetramethyltriphenyl-2,5,2',5'-tetracarboxylate (575.1 mg, 74.7%). <sup>1</sup>H NMR (600 MHz,  $\text{CDCl}_3$ )  $\delta$  8.13 (s, 2H), 8.08 (dd,  $J = 8.0, 1.4$  Hz, 2H), 7.88 (d,  $J = 8.0$  Hz, 2H), 7.39 (s, 4H), 3.96 (s, 6H), 3.71 (s, 6H). <sup>13</sup>C NMR (151 MHz,  $\text{CDCl}_3$ )  $\delta$  168.44 (s), 166.15 (s), 141.95 (s), 139.68 (s), 134.96 (s), 132.53 (s), 131.70 (s), 129.84 (s), 128.24 (d,  $J = 9.0$  Hz), 52.43 (s), 52.21 (s). <sup>13</sup>C NMR (151 MHz,  $\text{CDCl}_3$ )  $\delta$  168.44 (s), 166.15 (s), 141.95 (s), 139.68 (s), 134.96 (s), 132.53 (s), 131.70 (s), 129.84 (s), 128.24 (d,  $J = 9.0$  Hz), 52.43 (s), 52.21 (s).

#### **Synthesis of [1,1':4',1''-terphenyl]-2,2'',5,5''-tetracarboxylic acid (P-H<sub>4</sub>TT):**

S1(500.0 mg, 1.1 mmol) was then suspended in a mixture of THF (5.0 mL) and H<sub>2</sub>O (5.0 mL), to which 10.0 mL of 0.2 M NaOH aqueous solution was added. The mixture was stirred under reflux for 12 h and then cooled to room temperature. The THF was removed under a vacuum. Dilute HCl was added to the remaining aqueous solution until the solution was at pH = 3. The solid was collected by filtration, washed with water, and white powder was obtained (404.3 mg, 92.1%). <sup>1</sup>H NMR (600 MHz, DMSO)  $\delta$  13.28 (s, 4H), 8.01 (d,  $J = 7.9$  Hz, 2H), 7.94 (s, 2H), 7.84 (d,  $J = 7.9$  Hz, 2H), 7.47 (s, 4H). <sup>13</sup>C NMR (151 MHz, D<sub>2</sub>O)  $\delta$  171.81 (s), 169.16 (s), 142.89 (s),

141.82 (s), 138.99 (s), 135.38 (s), 133.72 (s), 132.03 (s), 130.88 (d,  $J = 16.5$  Hz). HR-MS (ESI): Calcd. for  $[M-H]^-$ : 405.0616, found: 405.0614.

**Synthesis of sodium [1,1':4',1''-terphenyl]-2,2'',5,5''-tetracarboxylate (P-TT):** To a stirred aqueous suspension (10.0 mL) of P-H<sub>4</sub>TT (400.0 mg, 1.0 mmol), an aqueous solution (5.0 mL) of NaOH (2.0 g, 5.0 mmol) was added at room temperature. After the completion of the reaction, the solution was filtered, and ethanol (15.0 mL) was added to the filtrate, resulting in white precipitates. The white precipitate obtained was filtered, washed with ethanol, and dried in air. Yield: 433.2 mg (89.1%). <sup>1</sup>H NMR (400 MHz, D<sub>2</sub>O)  $\delta$  7.83 (s, 2H), 7.75 (d,  $J = 7.8$  Hz, 2H), 7.48 (s, 4H), 7.42 (d,  $J = 7.8$  Hz, 2H). <sup>13</sup>C NMR (151 MHz, D<sub>2</sub>O)  $\delta$  178.50 (s), 175.14 (s), 141.79 (s), 139.91 (s), 137.64 (s), 136.46 (s), 130.29 (s), 128.43 (s), 127.72 (s), 126.76 (s).

**Synthesis of tetramethyl [1,1':3',1''-terphenyl]-2,2'',5,5''-tetracarboxylate(S2):** Dimethyl 2-bromoterephthalate (1000.0 mg, 3.7 mmol), 1,3-Phenylenediboronic Acid Pinacol Ester (562.3 mg, 1.7 mmol), and K<sub>2</sub>CO<sub>3</sub> (1446.5 mg, 8.3 mmol) were mixed in a 100 mL Schlenk flask. After added Pd(PPh<sub>3</sub>)<sub>2</sub>Cl<sub>2</sub> (58.2 mg, 0.1 mmol) in the glove box, then add anhydrous 1,4-dioxane (20.0 mL). The mixture was heated to reflux for a week under an Ar atmosphere. And then cooled to room temperature. After extraction with dichloromethane, the organic phases were combined, washed with water three times, and then dried over anhydrous sodium sulfate. The organic phase was removed in vacuo to yield the crude oily product. Then 30.0 mL of n-hexane was added, and it was allowed to stand for 24 h. After precipitation of the solid, it was washed with n-hexane and filtered. Recrystallization from methanol yields pure S2 (461.2 mg, 58.2% yield). <sup>1</sup>H NMR (600 MHz, CDCl<sub>3</sub>)  $\delta$  8.08 (d,  $J = 9.7$  Hz, 4H), 7.87 (d,  $J = 7.9$  Hz, 2H), 7.46 (t,  $J = 7.6$  Hz, 1H), 7.37 – 7.28 (m, 3H), 3.94 (s, 6H), 3.71 (s, 6H). <sup>13</sup>C NMR (151 MHz, CDCl<sub>3</sub>)  $\delta$  168.41 (s), 166.11 (s), 142.02 (s), 140.40 (s), 134.96 (s), 132.49 (s), 131.76 (s), 129.86 (s), 128.29 (d,  $J = 11.5$  Hz), 128.06 (s), 127.64 (s), 52.45 (s), 52.29 (s).

**Synthesis of [1,1':3',1''-terphenyl]-2,2'',5,5''-tetracarboxylic acid (M-H<sub>4</sub>TT):** S2 (450.0 mg, 1.0 mmol) was then suspended in a mixture of THF (5.0 mL) and H<sub>2</sub>O (5.0 mL), to which 10.0 mL of 0.2 M NaOH aqueous solution was added. The mixture was stirred under reflux for 12 h and then cooled to room temperature. The THF was removed under a vacuum. Dilute HCl was added to the remaining aqueous solution until the solution was at pH = 3. The solid was collected by filtration, washed with water, and white powder was obtained (351.9 mg, 89.2%). <sup>1</sup>H NMR (600 MHz, DMSO)  $\delta$  13.27 (s, 4H), 8.02 (d,  $J = 6.8$  Hz, 2H), 7.95 (s, 2H), 7.84 (d,  $J = 7.9$  Hz, 2H), 7.52 (t,  $J = 7.6$  Hz, 1H), 7.42 (d,  $J = 7.4$  Hz, 2H), 7.38 (s, 1H). <sup>13</sup>C NMR (151

MHz, DMSO)  $\delta$  169.60 (s), 166.97 (s), 140.85 (s), 140.31 (s), 136.75 (s), 133.20 (s), 131.51 (s), 129.82 (s), 128.86 (s), 128.68 (s), 128.50 (s), 128.07 (s). HR-MS (ESI): Calcd. for [M-H]<sup>-</sup>: 405.0616, found: 405.0622.

**Synthesis of sodium [1,1':3',1''-terphenyl]-2,2'',5,5''-tetracarboxylate (M-TT):** To a stirred aqueous suspension (10.0 mL) of P-H<sub>4</sub>TT (400.0 mg, 1.0 mmol), an aqueous solution (5.0 mL) of NaOH (2.0 g, 5.0 mmol) was added at room temperature. After the completion of the reaction, the solution was filtered, and ethanol (15.0 mL) was added to the filtrate, resulting in white precipitates. The white precipitate obtained was filtered, washed with ethanol, and dried in air. Yield: 317.6 mg (87.1%). <sup>1</sup>H NMR (600 MHz, D<sub>2</sub>O)  $\delta$  7.88 (s, 2H), 7.81 (d, *J* = 7.7 Hz, 2H), 7.58 (s, 1H), 7.47 (d, *J* = 8.8 Hz, 4H). <sup>13</sup>C NMR (151 MHz, D<sub>2</sub>O)  $\delta$  178.43 (s), 175.13 (s), 141.84 (s), 141.01 (s), 137.84 (s), 136.44 (s), 130.32 (s), 128.64 (s), 128.34 – 128.11 (m), 127.87 (d, *J* = 34.0 Hz), 127.45 (s), 126.71 (s).

## 2.2 Material characterizations:

The nuclear magnetic resonance (NMR) spectra were obtained from a BRUKER AVANCE III 600 MHz NMR Instrument (in CDCl<sub>3</sub>). Data for <sup>1</sup>H NMR are recorded as follows: chemical shift (ppm), multiplicity (s, singlet; d, doublet; t, triplet; q, quarter; m, multiple), coupling constant (Hz), integration. Data for <sup>13</sup>C NMR are reported in terms of chemical shift ( $\delta$ , ppm). JSM-7800F field emission scanning electron microscope was used to characterize morphology. The crystal structures were analyzed using MAXima-X XRD-7000. The Fourier transform infrared spectrometer (FT-IR) was recorded using KBr pellets on a Thermo Nicolet 6700 with the wavenumber range of 400-4000 cm<sup>-1</sup>. Transmission spectra were measured using a UV-Vis-NIR spectrophotometer (Agilent Cary 5000), the UCL spectra were measured using a fluorescence spectrophotometer (PerkinElmer LS55) equipped with a power-tunable 980 nm continuous wave laser diode (LD) as excitation source. The electric conductivity of the composite was measured by the four-probe method (Suzhou Jingge Electronics ST2643).

## 2.3 Electrochemical tests:

For the half cell, the working electrodes were prepared by casting the slurry onto a clean Al foil, where the slurry contained the active materials (70 wt%), carbon black (Super P, 20 wt%), and poly (vinylidene fluoride) binder (PVDF, 10 wt%). Then, the collector was dried overnight at 60 °C. The separator was Whatman glass fiber. The samples of electrochemically active materials were evaluated in 2032-type coin cells with a Na disk as the counter electrode and 1.0M NaCF<sub>3</sub>SO<sub>3</sub> (in TETRAGLYME=100 Vol%, Duoduo chemical reagent Co., LTD, Suzhou). The

average loading of active materials was 0.8~1.4 mg cm<sup>-2</sup>. All battery assembly and disassembly are performed in a dry Ar-filled glove box (H<sub>2</sub>O<0.1 ppm, O<sub>2</sub><0.1ppm Mikrouna).

The galvanostatic cycling test was carried on a CT-4008T instrument (Shen Zhen NEWARE electronic Co.). Cyclic voltammograms (CVs) were tested on a CHI instrument electrochemical workstation (Corrtest CS310H) at a scan rate of 0.1 mV s<sup>-1</sup> between 0.1 and 2.6 V (vs Na<sup>+</sup>/Na). The electrochemical impedance spectroscopy (EIS) test was measured by a CHI instrument electrochemical workstation in the frequency range of 10<sup>-2</sup>-10<sup>5</sup> Hz at the amplitude of 5 mV. All the tests were performed at room temperature.

#### 2.4 Calculate the number of Na<sup>+</sup> stored:

The theoretical specific capacity (C) of the sodium-ion batteries is calculated using the formula:

$$C = \frac{nF}{3.6 M} \dots (S1)$$

*n* is the number of sodium-ion transfer, *F* is the Faraday constant and *M* is the mole weight of the organic molecule.

#### 2.5 GITT test:

The Na<sup>+</sup> diffusion coefficient (*D*<sub>Na<sup>+</sup></sub>) was calculated by the galvanostatic intermittent titration technique measurement (GITT) method according to the following equation :

$$C = \frac{n}{V} = \frac{n}{n \cdot V_m} = \frac{1}{V_m} \dots (S2)$$

$$D_{Na^+} = \frac{4 \left( \frac{n_m V_m}{S} \right)^2 \left( \frac{\Delta E_s}{\tau (dE_t/d\sqrt{\tau})} \right)^2}{\pi \tau \left( \frac{n_m V_m}{S} \right)^2 \left( \frac{\Delta E_t}{\Delta E_s} \right)^2} \dots (S3)$$

where  $\tau$  is the pulse time,  $n_m$  is the mole number,  $V_m$  is the molar volume,  $S$  is the electrode-electrolyte interface area,  $\Delta E_s$  is the voltage difference between the steady-state and the initial state of every step, and  $\Delta E_t$  is the change of total voltage during a pulse step excluding the *IR* drop. The molar volume of per sample repetitive unit was calculated by measuring the mass and the total volume of a pressed sample pellet (Table S1), and the value was acceptable here when compared with some reported organic electrode materials. It is worth noting that the observed Na-ion diffusion coefficient of organic materials is usually higher than that of inorganic electrodes composited by ionic bonds, because the solid/crystalline state of organic materials is



mainly interacted by van der Waals forces, indicating that the organic material should be sodium Ion transmission provides greater void space.

Additionally, the Na<sup>+</sup> diffusion coefficient in the electrodes can be evaluated based on the low-frequency region of EIS according to the following equations:

$$D_{Na^+} = \frac{R^2 T^2}{2n^2 A^2 F^4 C^2 \sigma^2} = \frac{R^2 T^2}{2n^2 A^2 F^4 \left(\frac{1}{V_m}\right)^2 \sigma^2} = \frac{R^2 T^2 V_m}{2n^2 A^2 F^4 \sigma^2} \dots\dots (S4)$$

$R$  represents the universal gas constant,  $T$  is the absolute temperature (room temperature).  $A$  corresponds to the area of the electrode,  $n$  denotes the charge number,  $F$  refers to the Faraday constant,  $C$  represents the molar concentration of Na-ion.  $\sigma$  is the slope of the line  $Z' \sim \omega^{-1/2}$  which can be obtained from the line of  $Z' \sim \omega^{-1/2}$ , respectively. Deduction process is provided in Eq. S3.

$$Z' = R + \sigma \omega^{-1/2} \quad (S5)$$

$$Z' = R_s + R_{ct} + \sigma_w \omega^{-\frac{1}{2}} \dots\dots (S6)$$

where  $R_s$  and  $R_{ct}$  represent the charge transfer resistance and the solution resistance, respectively.

In addition, the diffusion coefficient of sodium ions ( $D_{Na^+}$ ) can be estimated based on the following formula:

$$D_{Na^+} = \frac{R^2 T^2}{2n^4 F^4 \sigma_w^2 A^2 C^2} \dots\dots (S7)$$

In the two formulas,  $R$ ,  $T$ ,  $N$ ,  $F$ ,  $A$ , and  $C$  represent the gas constant, absolute temperature, number of electrons transferred per unit of material during the electrochemical reaction during the reaction, Faraday's constant, the surface area of the working electrode, and the concentration of sodium ions;  $R_s$  and  $R_{ct}$  represent solution resistance and charge transfer resistance, respectively.

## 2.6 Calculate methods and details of capacitive effect contribution and diffusion-controlled contribution :

$$i = a v^b \quad (S8)$$

Where  $a$  and  $b$  are the adjustable parameters,  $b$ -value equal to 1 indicates charge storage is entirely from the capacitive-controlled process while a  $b$ -value of 0.5 signifies a total diffusion-controlled reaction.

Using the scan-rate-dependent CV curves (Fig. 5a,c) to quantify the contribution from capacitive effects (both surface pseudocapacitance and doublelayer capacitance) and diffusion-controlled  $\text{Na}^+$  insertion process to the current response according to the following Equation S8;

$$I(v) = k_1 v + k_2 v^{\frac{1}{2}} \quad (\text{S9})$$

Where  $I(v)$ ,  $k_1 v$  and  $k_2 v^{1/2}$  represent the total current response at a given potential  $V$ , current due to surface capacitive effects, and current due to diffusion-controlled  $\text{Na}^+$  insertion process, respectively. The above equation can also be reformulated as Equation S9;

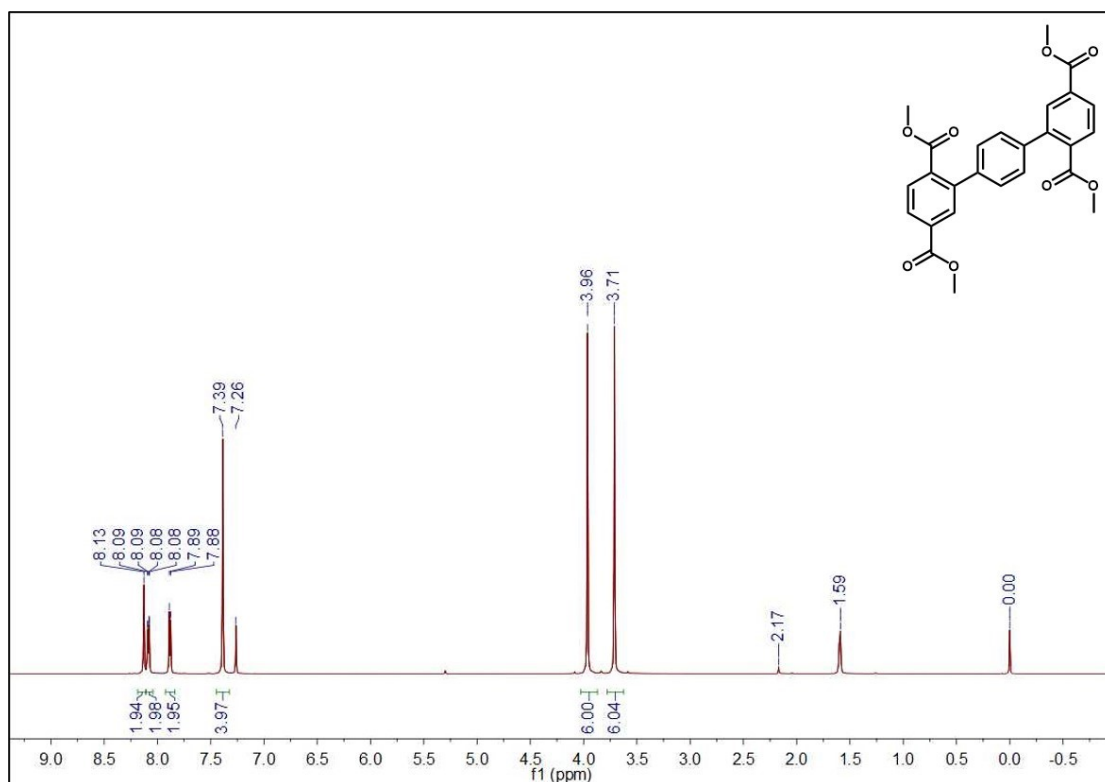
$$I(v)/v^{\frac{1}{2}} = k_1 v^{\frac{1}{2}} + k_2 \quad (\text{S10})$$

By plotting  $I(v)/v^{\frac{1}{2}}$  vs.  $v^{\frac{1}{2}}$  at different potentials, we can calculate the values of  $k_1$  (slope) and  $k_2$  (intercept) from the straight lines. After integration of the enclosed CV area, the amount of stored charge from different energy storage modes can be distinguished, expressed by the following Equation S10;

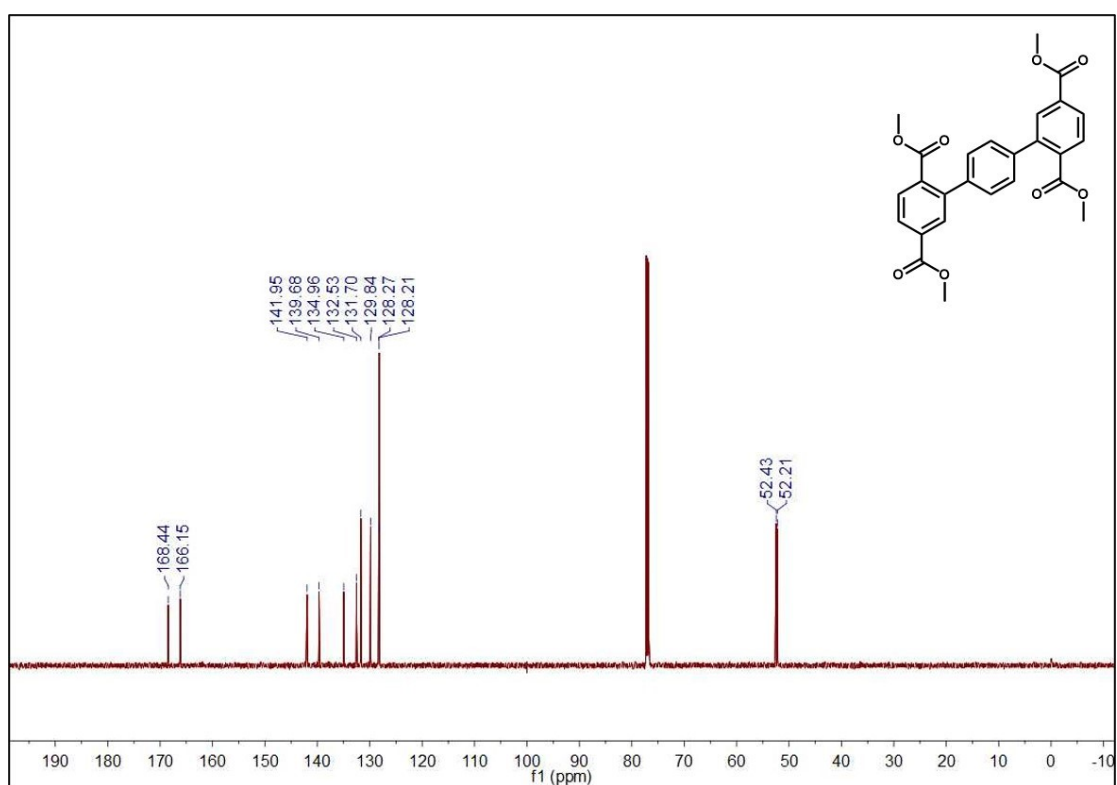
$$Q = Q_s + Q_d \quad (\text{S10})$$

Where,  $Q$ ,  $Q_s$ , and  $Q_d$  represent the total stored charge included in the enclosed CV area at set scan rate, surface capacitive effects, and diffusion-controlled  $\text{Na}^+$  insertion process, respectively.

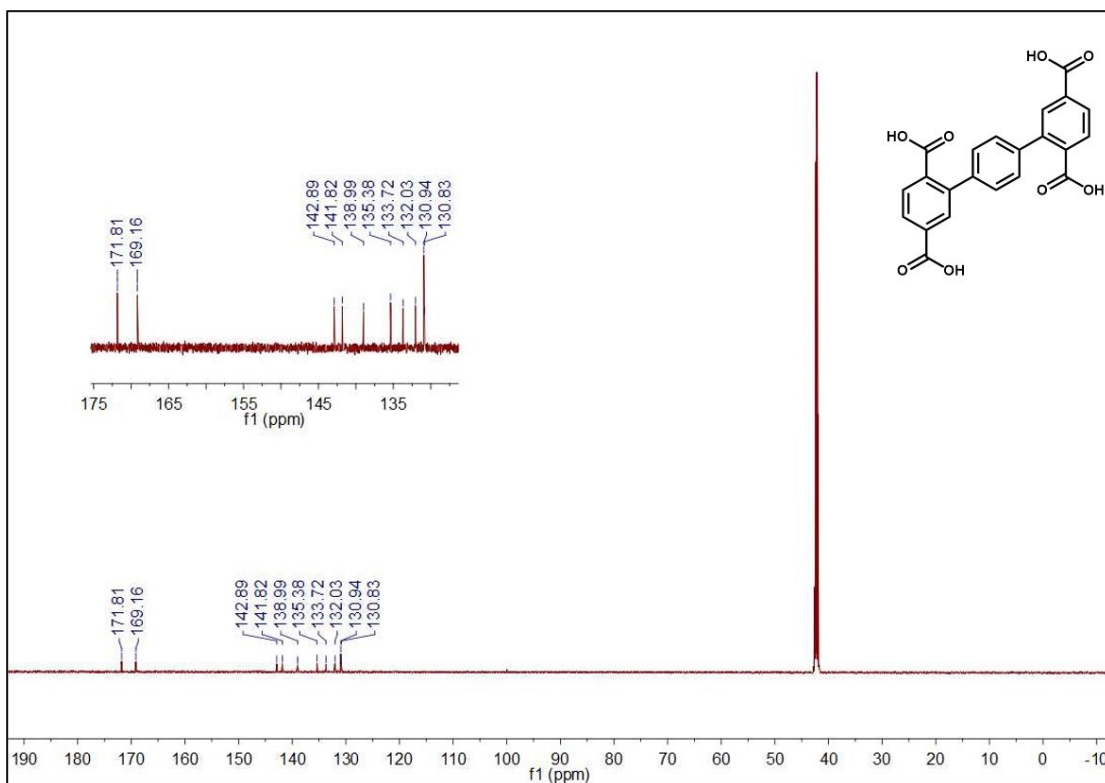
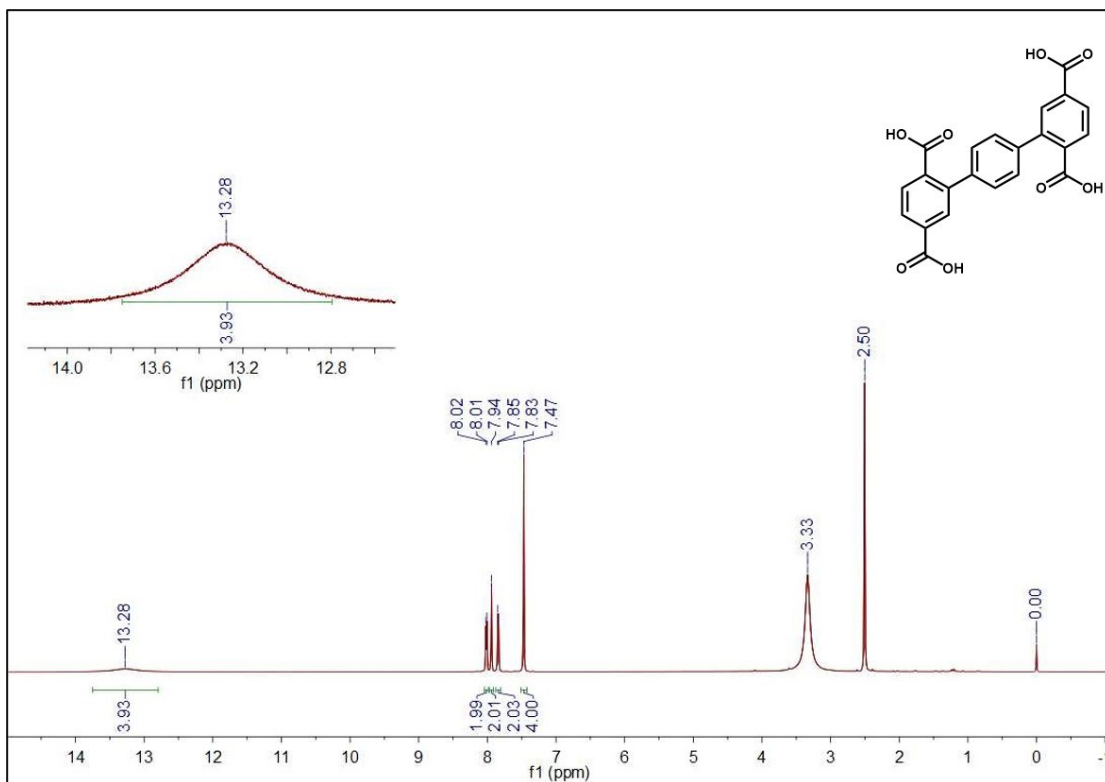
### 3. Spectra:



**Fig. S1.** <sup>1</sup>H NMR spectrum of S1 in CDCl<sub>3</sub>.



**Fig. S2.** <sup>13</sup>C NMR spectrum of S1 in CDCl<sub>3</sub>.



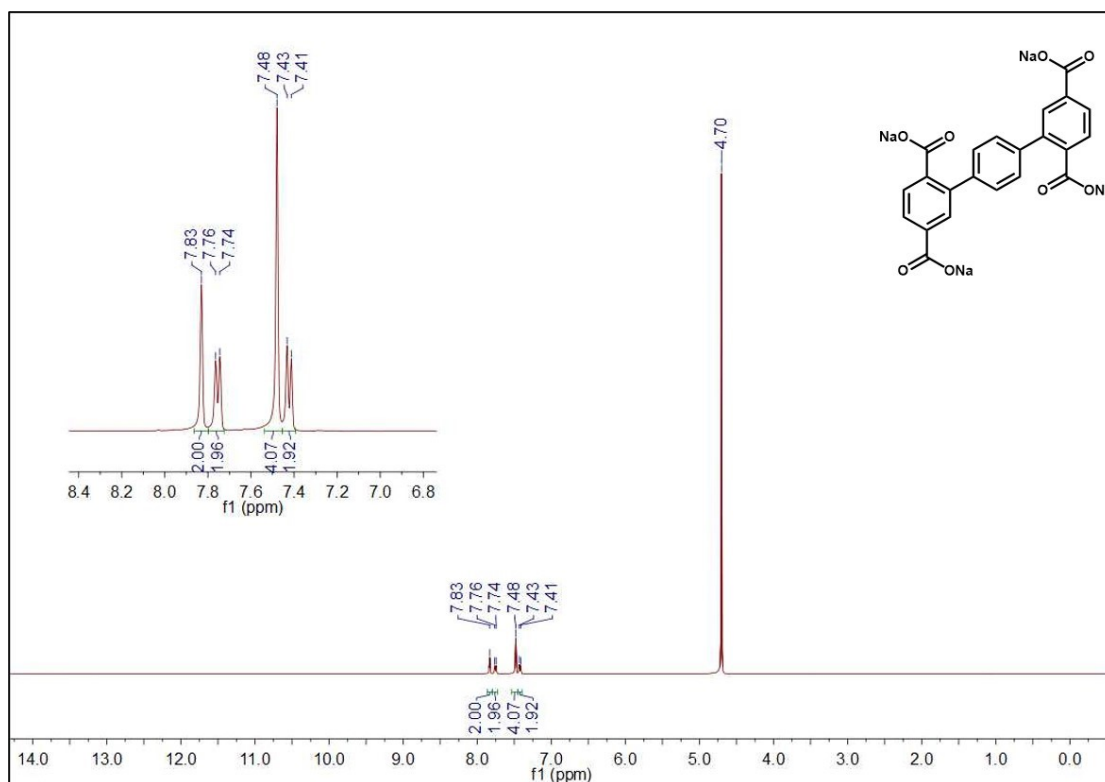


**Fig. S5.**  $^1\text{H}$  NMR spectrum of P-TT in  $\text{D}_2\text{O}$ .

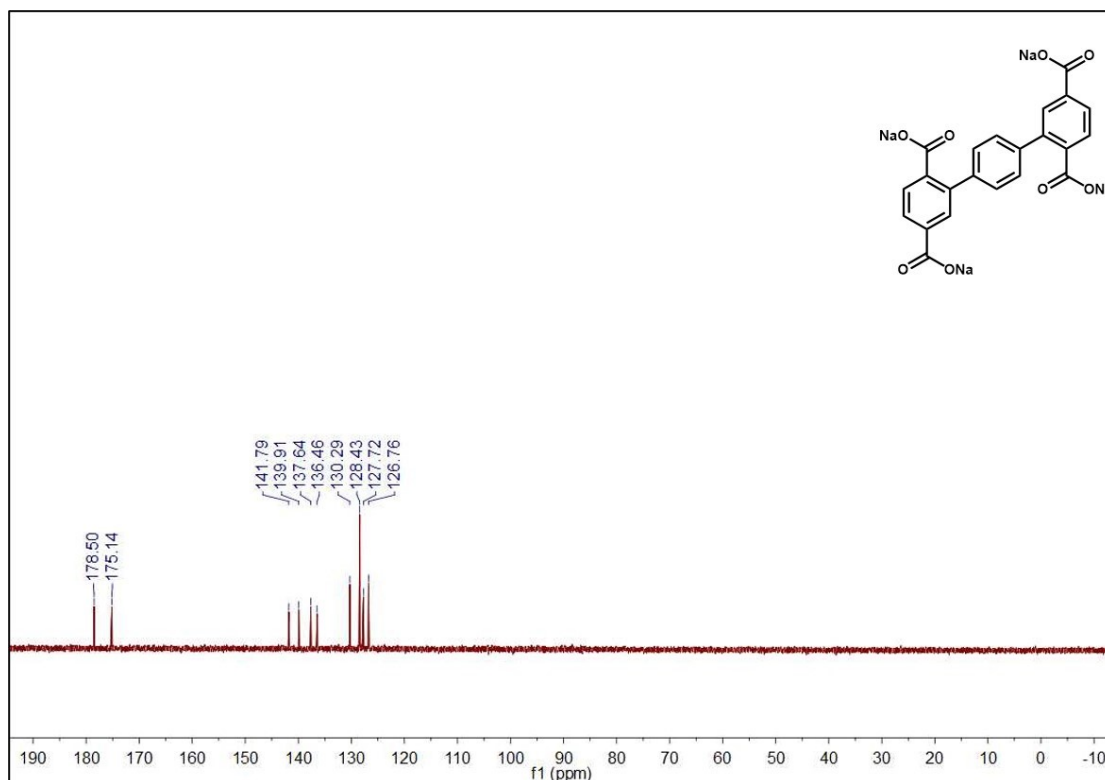


**Fig. S6.**  $^{13}\text{C}$  NMR spectrum of P-TT in  $\text{D}_2\text{O}$ .

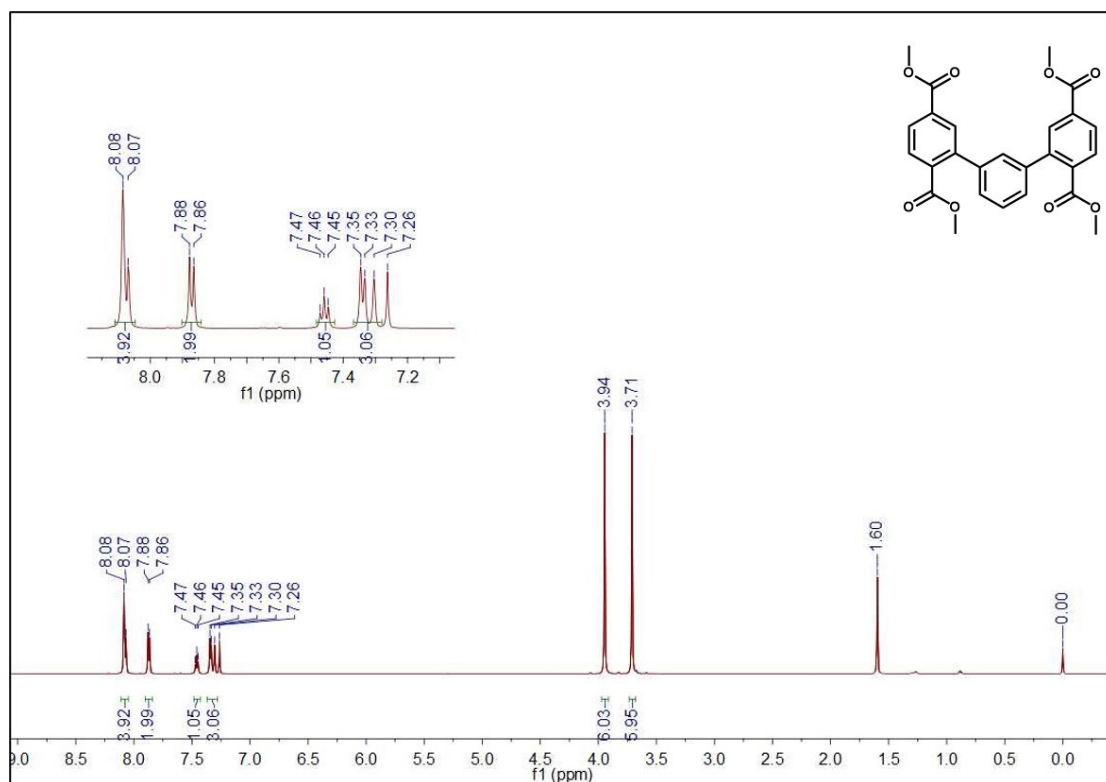


**Fig. S7.** <sup>1</sup>H NMR spectrum of S2 in CDCl<sub>3</sub>.

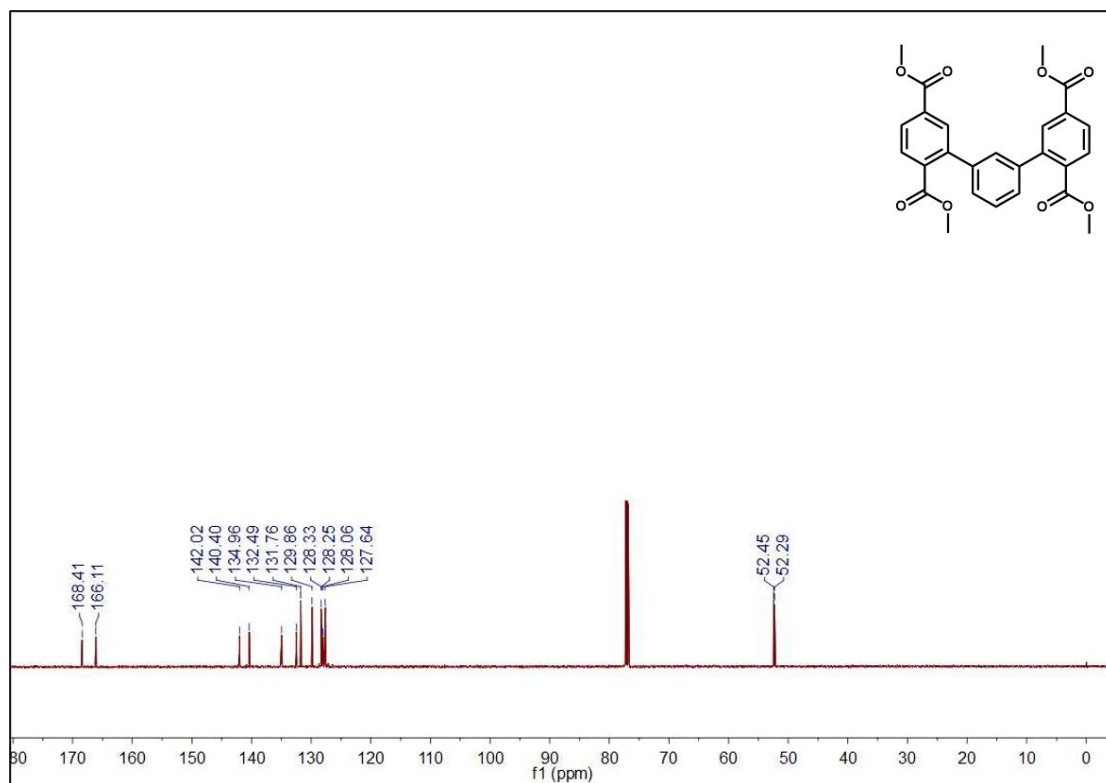


**Fig. S8.** <sup>13</sup>C NMR spectrum of S2 in CDCl<sub>3</sub>.

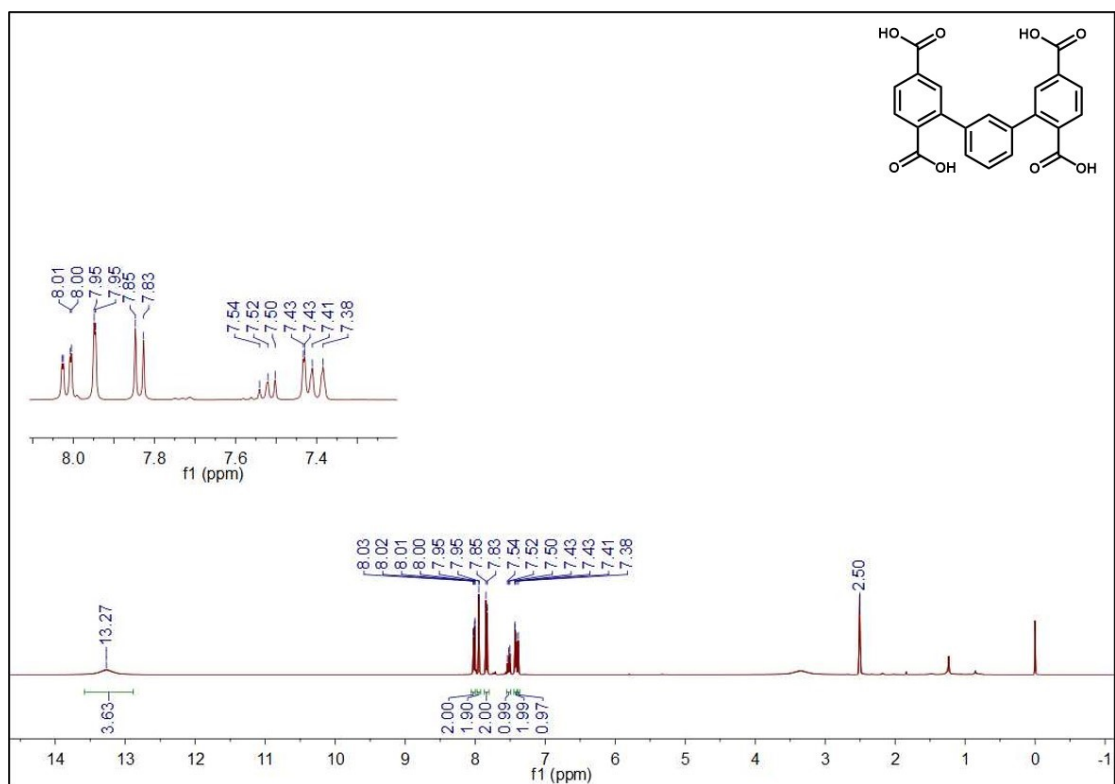


**Fig. S9.** <sup>1</sup>H NMR spectrum of M-H<sub>4</sub>TT in DMSO.

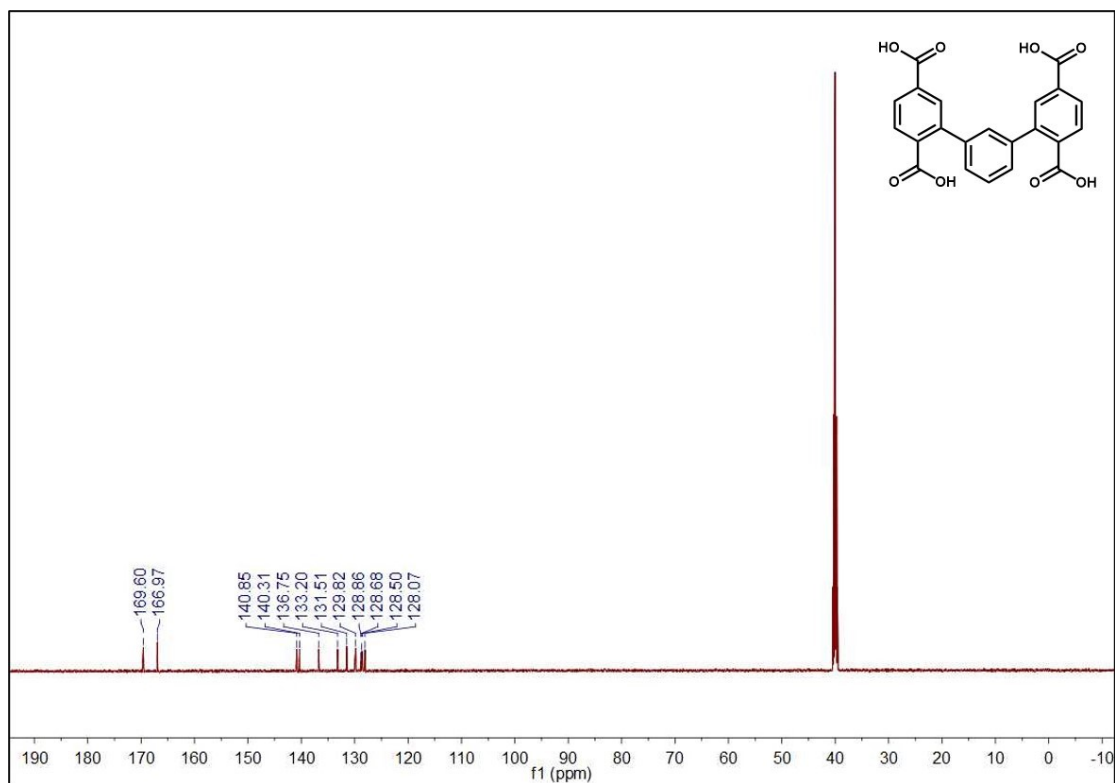


**Fig. S10.** <sup>13</sup>C NMR spectrum of M-H<sub>4</sub>TT in DMSO.

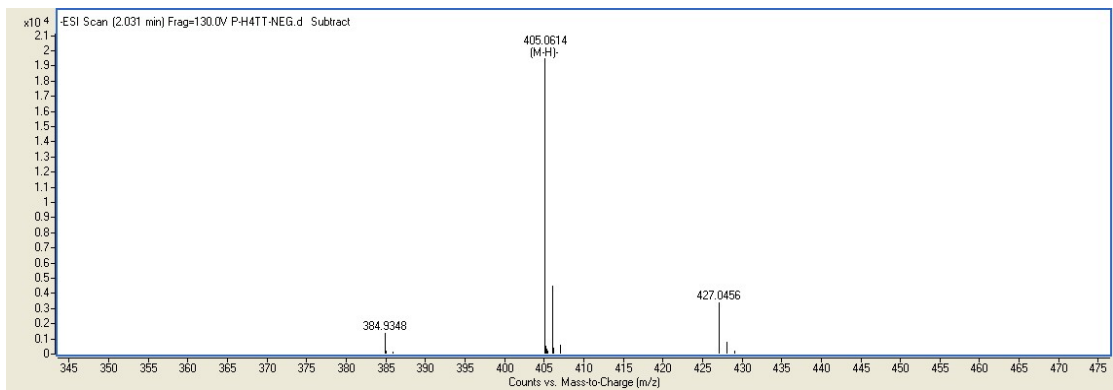


**Fig. S11.** ESI-MS of P-H<sub>4</sub>TT.

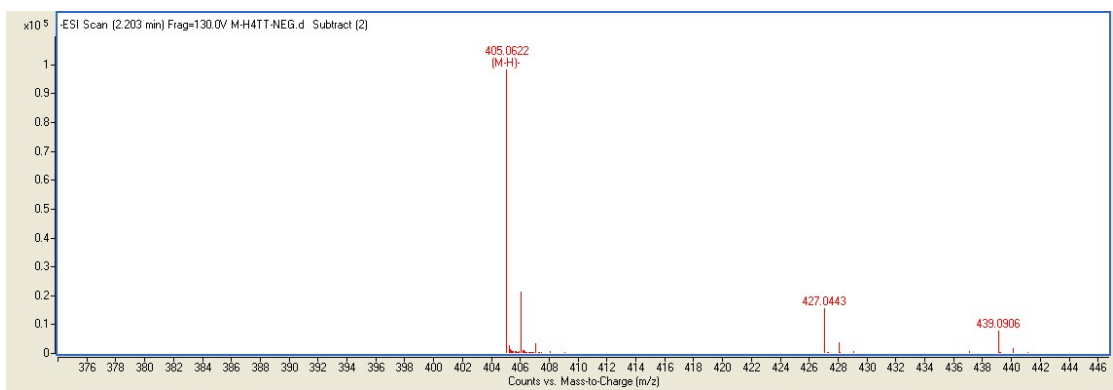


**Fig. S12.** ESI-MS of M-H<sub>4</sub>TT.

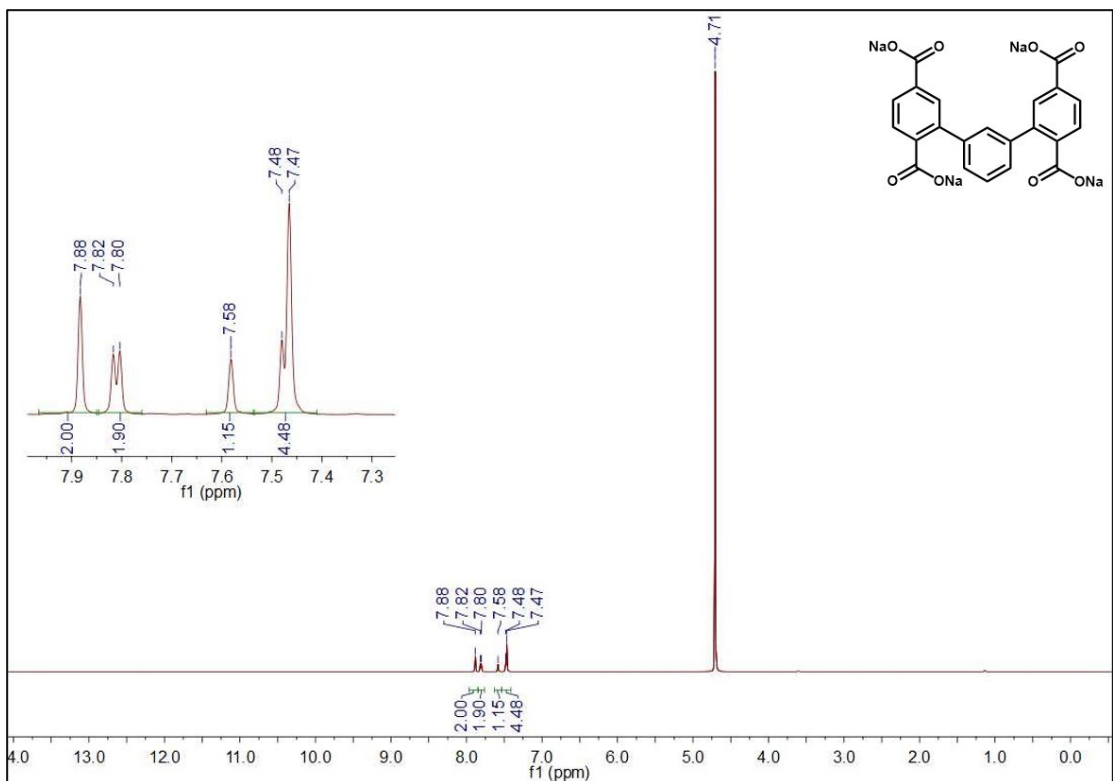




Fig. S13.  $^1\text{H}$  NMR spectrum of M-TT in  $\text{D}_2\text{O}$ .

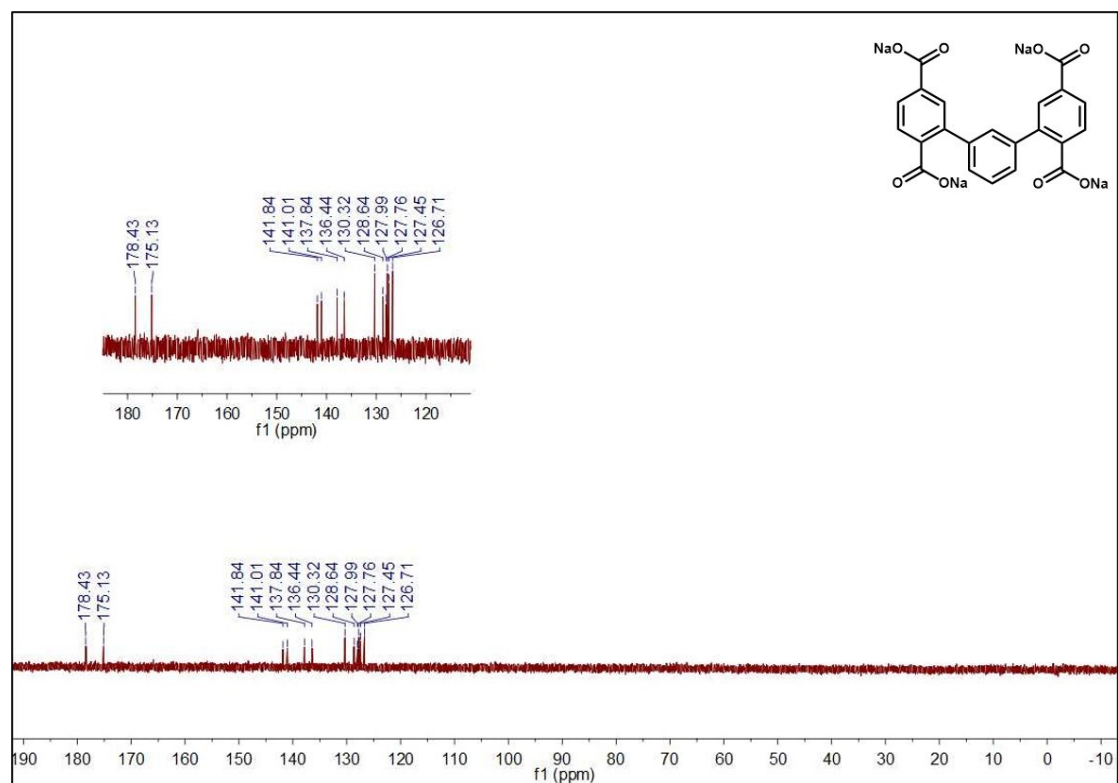
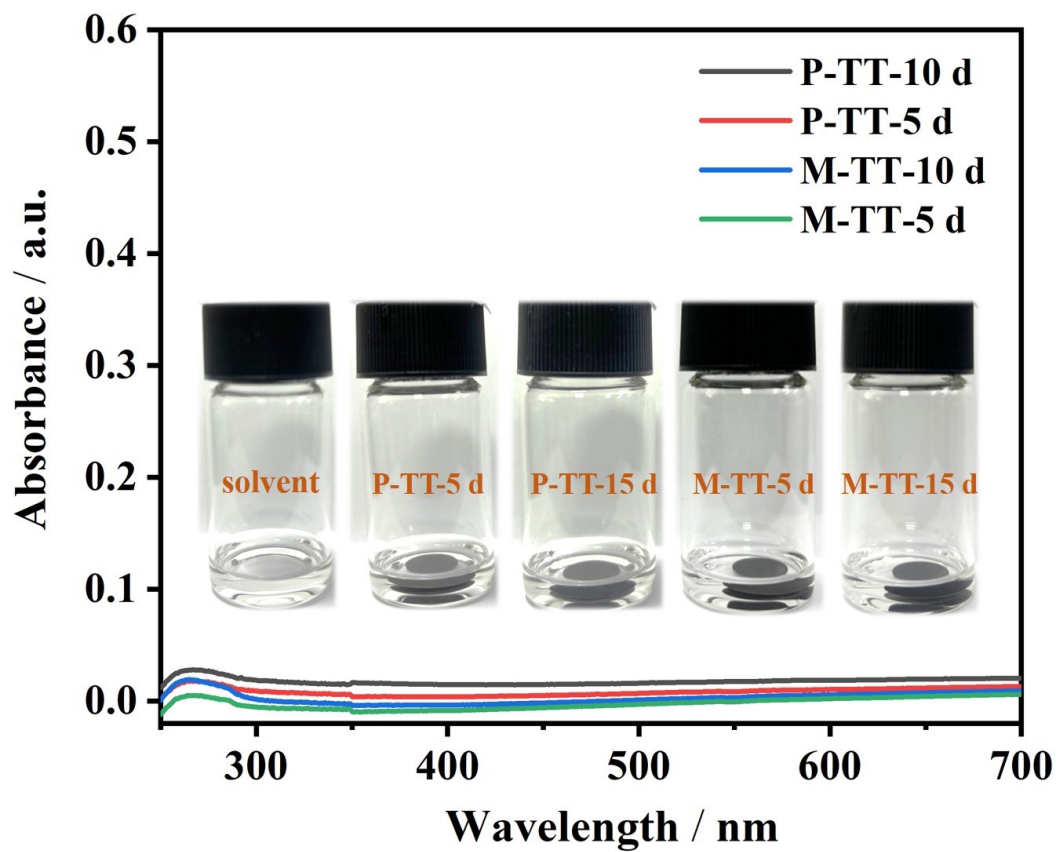
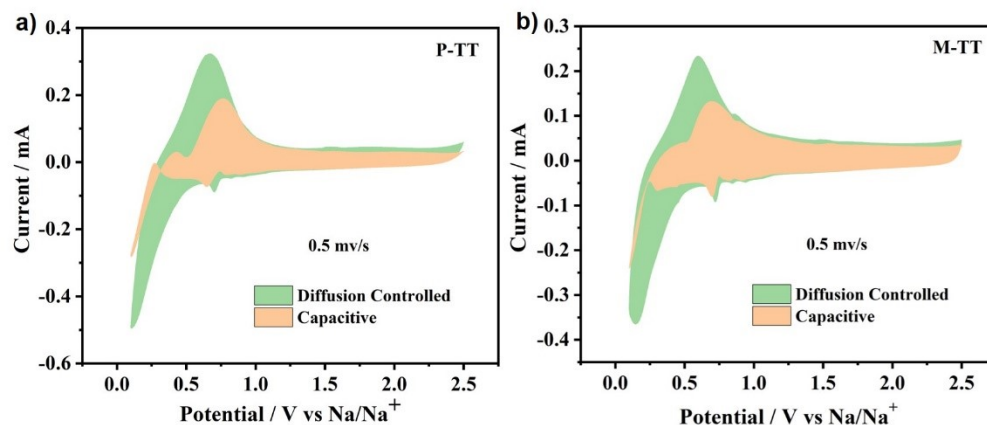


Fig. S14.  $^{13}\text{C}$  NMR spectrum of M-TT in  $\text{D}_2\text{O}$ .



**Fig. S15.** The UV-vis absorption spectra of M-TT and P-TT (solvent, TETRAGLYME=100 Vol%, 25 °C); insets: photographs of M-TT and P-TT electrode-immersed solvents of TETRAGLYME on different days.



**Fig. S16.** CV curve of a) P-TT and b) M-TT with the pseudocapacitive contribution shown by the shaded regions at a scan rate of 0.5 mV s<sup>-1</sup>.



**Fig. S17.** The P-TT pellet was obtained by the classic powder's pressing method (18 MPa).

The weight, thickness and diameter of the resulting pellet were 136.4 mg, 0.677 mm, and 13.050 mm, respectively. The molar volume ( $V_m$ ) of the repeating unit of sample is about 327.9 cm<sup>3</sup> mol<sup>-1</sup>.



**Fig. S18.** The M-TT pellet was obtained by the classic powder pressing method (18 MPa).

The M-TT pellet was obtained by classic powder pressing method (18 MPa). The weight, thickness, and diameter of the resulting pellet were 111.6 mg, 0.571 mm, and 13.042 mm, respectively. The molar volume ( $V_m$ ) of the repeating unit of sample is about  $337.8 \text{ cm}^3 \text{ mol}^{-1}$ .

Material	Electric conductivity (mS/cm)
M-TT	$3.8 \times 10^{-4} \sim 4.2 \times 10^{-4}$
P-TT	$3.1 \times 10^{-4} \sim 3.7 \times 10^{-4}$

**Table S1.** Electric conductivity results of M-TT and P-TT.

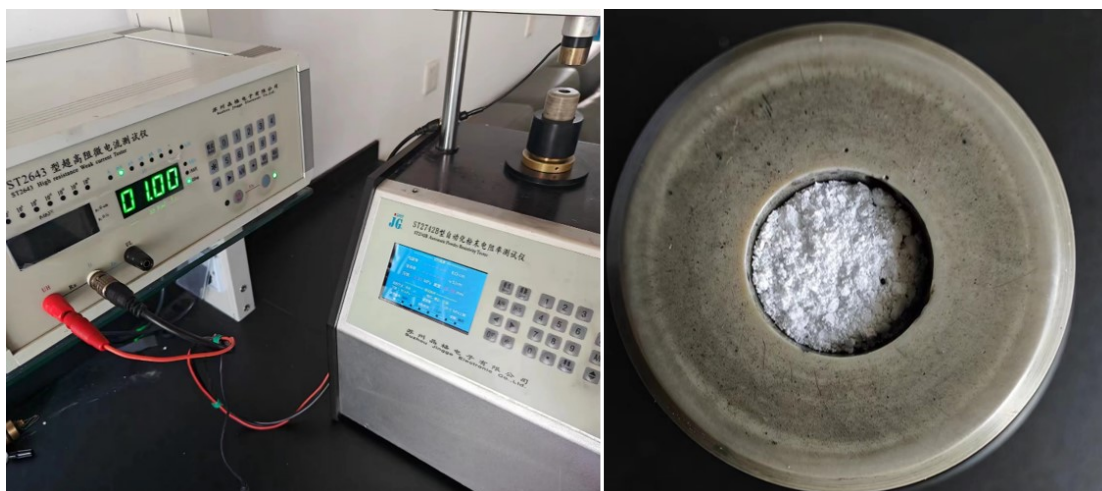


**Fig. S19** The electric conductivity of the composite was measured by the four-probe method (Suzhou Jingge Electronics ST2643).